tion of the nosetip with 50 μ-in. roughness and indicate that transition had occurred at a Reynolds number of approximately 1.8×10^6. These results provide additional evidence of nosetip threshold conditions that determine when the nosetip would produce low frustum transition Reynolds numbers. This example also illustrates a case of unsteady transition location for this early frustum transition condition. Transition steadily moved rearward with increasing time and in 2.5 s both sides of the model had a completely laminar boundary layer. (The time interval for each sequence of data is indicated. As shown, $t=0$ is the time when the model arrived at the tunnel centerline.)

It was interesting to relate the transition reversal results of Refs. 3 and 4 to these present findings. An estimate of the sonic point conditions for the experiments of both references indicated they were close to the threshold conditions for the case of nosetip-instability-dominated frustum transition. This suggests the possibility that these transition data were not really a transition reversal resulting from frustum surface temperature changes, but may have resulted from nosetip instabilities.

References

[1]Lees, L., "The Stability of the Laminar Boundary Layer in a Compressible Fluid," NACA Rept. 876, 1947.

[2]Van Driest, E. R., "Calculations of the Stability of the Laminar Boundary Layer in a Compressible Fluid on a Flat Plate With Heat Transfer," *Journal of Aeronautical Sciences,* Vol. 19, Dec. 1952, pp. 801–812, 828.

[3]Jack, J. R., Wisniewski, R. J., and Diaconis, N. S., "Effect of Extreme Surface Cooling on Boundary Layer Transition," NACA TN-4094, Oct. 1957.

[4]Muir, J. R. and Trujillo, A. A., "Experimental Investigation of the Effects of Nose Bluntness, Free-Stream Unit Reynolds Number, and Angle of Attack on Cone Boundary Layer Transition at a Mach Number of 6," AIAA Paper 72-216, Jan. 1972.

[5]Stetson, K. F., "Effect of Bluntness and Angle of Attack on Boundary Layer Transition on Cones and Biconic Configurations," AIAA Paper 79-0269, Jan. 1979.

[6]Stetson, K. F., "Hypersonic Boundary Layer Transition Experiments," AFWAL-TR-80-3062, Oct. 1980.

[7]Stetson, K. F., "Nosetip Bluntness Effects on Cone Frustum Boundary Layer Transition in Hypersonic Flow," AIAA Paper 83-1763, July 1983.

[8]Fiore, A. W. and Law, C. H., "Aerodynamic Calibration of the Aerospace Research Laboratories M=6 High Reynolds Number Facility," ARL-TR-75-0028, Feb. 1975.

[9]Anderson, A. D., "Interim Report, Passive Nosetip Technology (PANT) Program, Vol. X, Appendix, Boundary Layer Transition on Nosetips With Rough Surfaces," Space and Missile Systems Organization, SAMSO-TR-74-86, Jan. 1975.

[10]Demetriades, A., "Nosetip Transition Experimentation Program, Final Report, Vol.2," Space and Missile Systems Organization, SAMSO-TR-76-120, July 1977.

Effects of Transverse Curvature on Oscillatory Flow Along a Circular Cylinder

Y. T. Chew*
National University of Singapore, Singapore
and
C. Y. Liu†
Nanyang Technological Institute, Singapore

Received Oct. 22, 1987; revision received Feb. 19, 1988.

*Associate Professor, Department of Mechanical and Production Engineering. Member AIAA.

†Professor, School of Mechanical and Production Engineering. Member AIAA.

Introduction

OSCILLATORY flows with zero mean velocity can be found in a variety of natural phenomena. The classic example of oscillatory flows in unbounded stagnant fluid is that over an infinite flat plate executing periodic sinusoidal motion along its plane. This was solved by Stokes[1] and is often referred to in the literature as Stokes flow. Some characteristic features of this flow are that, although the flow oscillates at the same frequency as the plate, it lags behind the plate, and the phase lag is proportional to the distance from the plate. The layer of oscillatory flow also is referred to in the literature as "Stokes layer."[2] Although there are not many engineering problems that can be classified as Stokes flow, it should be noted that Stokes layers can be embedded in other flowfields with almost independent properties. An example of this is in unsteady laminar boundary-layer flow. Lighthill[3] found mathematically that at large frequency of unsteadiness, a Stokes layer with profiles independent of the profiles of the steady layer is generated. Unsteady laminar boundary-layer flow has engineering application in the design of turbine and compressor blades where the flow along the blade is subjected to disturbances caused by the wake of preceding row of blades.

In the present Note, a general oscillatory Stokes flow including the transverse curvature effect is presented.

Analysis

It is assumed that a circular cylinder of radius a is of infinite length and oscillates azimuthally in a stationary, unbounded, incompressible Newtonian fluid. The equation of motion in cylindrical coordinates can be reduced to

$$\frac{\partial u}{\partial t}=\nu\left(\frac{\partial^2 u}{\partial r^2}+\frac{1}{r}\frac{\partial u}{\partial r}\right) \tag{1}$$

and the boundary conditions are

$$r=a,\ u=U_0\cos\omega t \quad \text{and} \quad r=\infty,\ u=0$$

where ν is the kinematic viscosity and ω the angular frequency.

Equation (1) is a linear, second-order partial differential equation. It can be solved by separation of variables. Assuming

$$u(r,t)=P(r)Q(t) \tag{2}$$

the solutions of functions Q and P are

$$Q=Ae^{i\omega t} \tag{3}$$

$$P=BI_0(\sqrt{i\omega/\nu}\,r)+CK_0(\sqrt{i\omega/\nu}\,r) \tag{4}$$

where A, B, and C are constants, I_0 and K_0 are modified zero-order Bessel function of first and second kind, respectively. The function I_0 does not converge when $r\to\infty$; thus, B must be equal to zero in order to satisfy the boundary condition.

The solution of Eq. (1) subjected to the boundary conditions can then be written as

$$u(r,t)=U_0\left[\frac{\mathrm{ker}_0(ka)\mathrm{ker}_0(kr)+\mathrm{kei}_0(ka)\mathrm{kei}_0(kr)}{\mathrm{ker}_0^2(ka)+\mathrm{kei}_0^2(ka)}\cos\omega t\right.$$

$$\left.+\frac{\mathrm{kei}_0(ka)\mathrm{ker}_0(kr)-\mathrm{ker}_0(ka)\mathrm{kei}_0(kr)}{\mathrm{ker}_0^2(ka)+\mathrm{kei}_0^2(ka)}\sin\omega t\right] \tag{5}$$

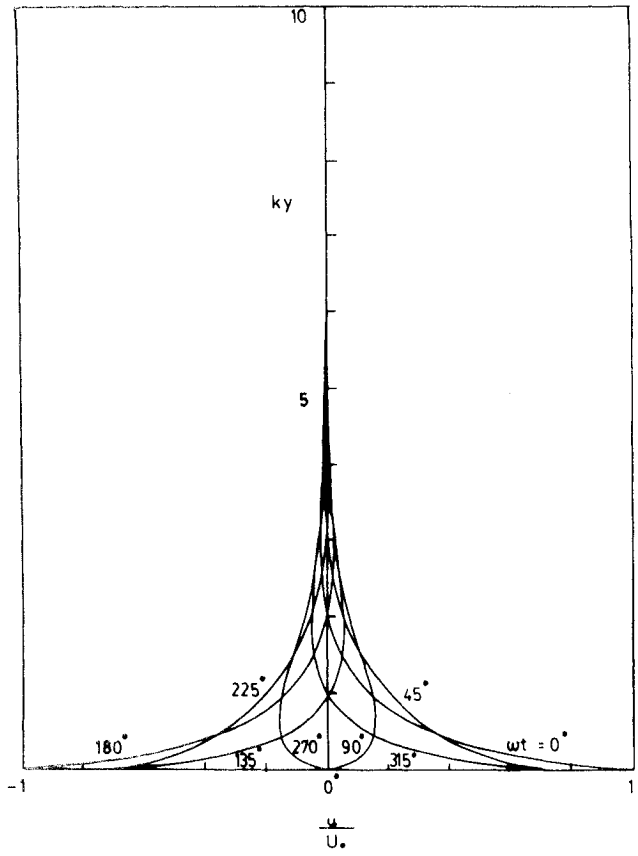

Fig. 1a Velocity profiles ($ka = 0.1$).

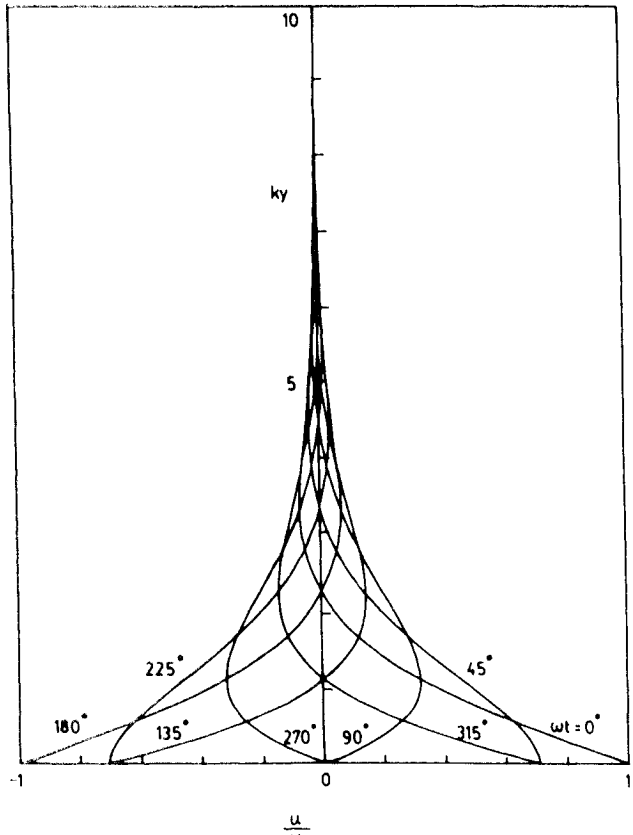

Fig. 1b Velocity profiles ($ka = 100$).

where $k = \sqrt{\omega/\nu}$.

Writing

$$N_0(kr) = \sqrt{\mathrm{ker}_0^2(kr) + \mathrm{kei}_0^2(kr)}$$

$$\cos\phi_0 = \frac{\mathrm{ker}_0(kr)}{N_0(kr)}$$

$$\sin\phi_0 = \frac{\mathrm{kei}_0(kr)}{N_0(kr)}$$

$$\varphi_0 = \phi_0(ka)$$

Equation (5) can be rewritten as

$$u(r,t) = U_0[N_0(kr)/N_0(ka)]\cos(\omega t + \phi_0 - \phi_0) \tag{6}$$

where $U_0[N_0(kr)/N_0(ka)]$ is the velocity amplitude of oscillation and $\phi_0 - \phi_0$ the phase angle. Both the velocity amplitude and phase angle are functions of the distance from the surface of the cylinder.

The skin-friction coefficient can be obtained by determining the velocity gradient at the wall and is given by

$$C_f = (\tau_w / \tfrac{1}{2}\rho U_0^2)$$

$$= (2/kA)\,[N_1(ka)/N_0(ka)]\cos(\omega t + \varphi_1 - \varphi_0) \tag{7}$$

where A is the amplitude of oscillation, i.e., $U_0 = A\omega$, and

$$N_1(kr) = \sqrt{\mathrm{ker}_0'^2(kr) + \mathrm{kei}_0'^2(kr)}$$

$$\cos\phi_1 = [\mathrm{ker}_0'(kr)/N_1(kr)]$$

$$\sin\phi_1 = [\mathrm{kei}_0'(kr)/N_1(kr)]$$

$$\varphi_1 = \phi_1(ka)$$

Results and Discussion

The velocity profiles were calculated from Eq. (6) numerically and plotted against ky, where $y = r - a$ for two different values of ka at various phases of oscillation ωt in Figs. 1a and 1b. The figures show that the velocity profile has the form of a damped harmonic oscillation with a velocity amplitude of $U_0 N_0(kr)/N_0(ka)$ and a phase lag of $(\varphi_0 - \phi_0)$ with respect to the motion of the wall. The damping increases with decreasing ka. This is also evident in the plot of velocity amplitude against ky for various ka in Fig. 2. The increase in damping generates a steeper velocity gradient at the wall resulting in higher wall shear stress that opposes the oscillatory motion of the cylinder.

The limiting case of the present analysis, when the radius of cylinder is infinitely large, is the oscillatory motion of a flat plate. Thus, the classical Stokes flow is a special case of the present more general analysis, and Eq. (6) can be shown to reduce to

$$u(y,t) = U_0 e^{-(k/\sqrt{2})y}\cos\left(\omega t - \frac{k}{\sqrt{2}}y\right) \tag{8}$$

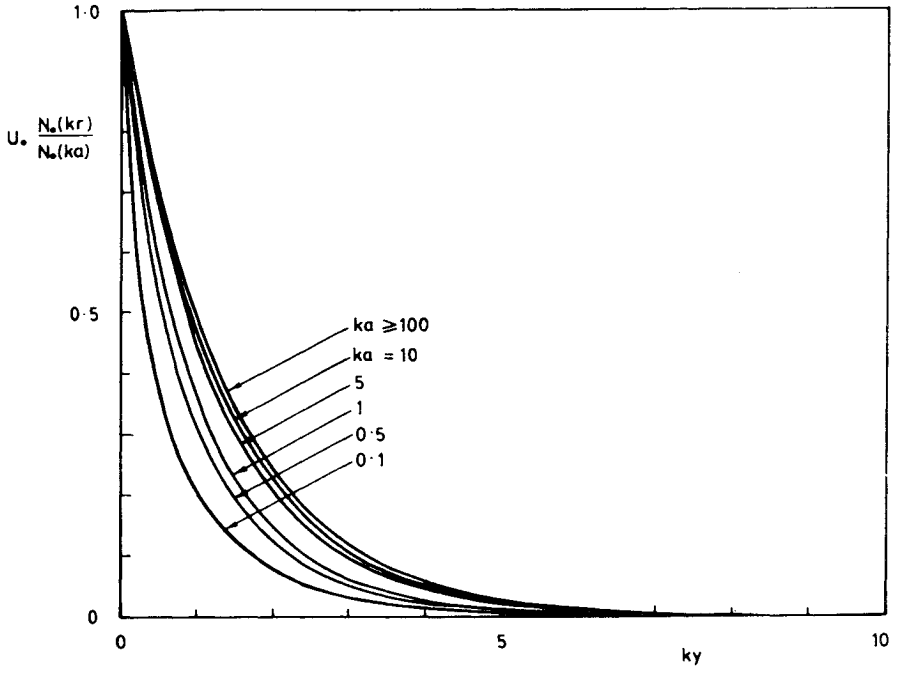

Fig. 2 Variation of velocity amplitude with ky.

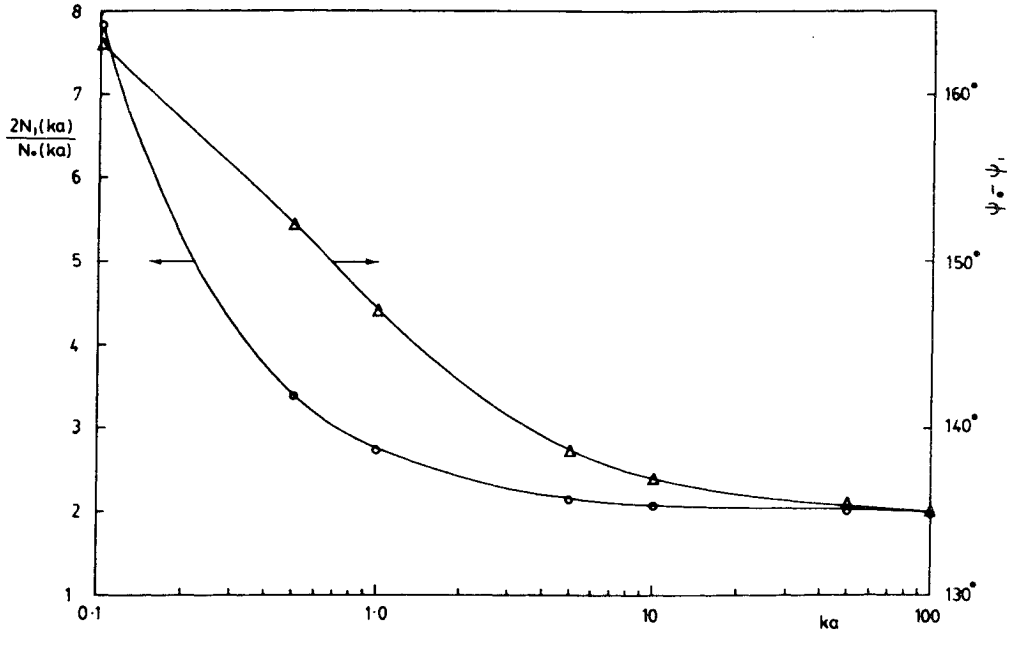

Fig. 3 Effect of transverse curvature on C_f amplitude and phase angle at $kA = 1$.

for the oscillatory flat plate. This verifies that the present theoretical analysis is sound.

The amplitude of the skin-friction coefficient C_f and the phase-lag angle $(\varphi_0 - \varphi_1)$ in Eq. (7) were calculated numerically and plotted against ka in Fig. 3 for the case of $kA = 1$. For oscillatory flat-plate motion, it can be deduced from Stokes flow that C_f is 2, and it lags behind the oscillatory motion of the wall by 135 deg. Figure 3 shows that C_f and $(\varphi_0 - \varphi_1)$ in the present flow approach the flat-plate values asymptotically when $ka \geq 100$. They also increase with decreasing ka.

Conclusions

The above analysis shows that the effects of transverse curvature are to increase the damping of velocity amplitude and skin friction in Stokes flow. They can only be neglected for $ka \geq 100$. Thus, in calculating the unsteady laminar boundary-layer flow along a circular cylinder, the transverse curvature effects must be considered.

References

[1] Stokes, G. G., "On the Effect of the Internal Friction of Fluids on the Motion of Pendulum," *Transactions of the Cambridge Philosophical Society,* Vol. 9, Pt. II, 1851, pp. 8–106.

[2] Telionis, D. P., *Unsteady Viscous Flows,* Springer-Verlag, New York, 1981, pp. 154–185.

[3] Lighthill, M. J., "The Response of Laminar Skin Friction and Heat Transfer to Fluctuations in the Stream Velocity," *Proceedings of the Royal Society of London, Series A,* Vol. 224, 1954, pp. 1–23.